Ab Initio Simulations for the Ion-Ion Structure Factor of Warm Dense Aluminum

Hannes R. Rüter and Ronald Redmer
Universität Rostock, Institut für Physik, D-18051 Rostock, Germany
(Received 11 December 2013; published 11 April 2014)

We perform *ab initio* simulations based on finite-temperature density functional theory in order to determine the static and dynamic ion-ion structure factor in aluminum. We calculate the dynamic structure factor via the intermediate scattering function and extract the dispersion relation for the collective excitations. The results are compared with available experimental x-ray scattering data. Very good agreement is obtained for the liquid metal domain. In addition we perform simulations for warm dense aluminum in order to obtain the ion dynamics in this strongly correlated quantum regime. We determine the sound velocity for both liquid and warm dense aluminum which can be checked experimentally using narrow-bandwidth free electron laser radiation.

DOI: 10.1103/PhysRevLett.112.145007 PACS numbers: 52.65.Yy, 52.25.−b, 52.35.Dm, 61.20.−p

A consistent description of dense charged particle systems is one of the major challenges of statistical mechanics [1]. While dilute Coulomb systems such as low-density plasmas or electrolytes at low concentrations can be treated appropriately within expansion techniques (e.g., with respect to density or fugacity), the investigation of dense plasmas has to deal with strong correlations and quantum effects; i.e., perturbative treatments or expansions with respect to small parameters are no longer applicable. A prime example for such complex states is warm dense matter (WDM)—a dense plasma with strong ion-ion correlations and at least partially degenerate electrons. This particular state is of paramount importance for astrophysics, e.g., for the interior of giant planets [2,3], and for inertial confinement fusion research [4].

Besides the equation of state data and the transport properties, the dynamic structure factor (DSF) $S(\vec{k},\omega)$ as the spectral function of the density-density correlations in the system is of fundamental importance. It is closely connected with the dielectric function via the fluctuation-dissipation theorem and, in principle, all other quantities can be derived from the DSF. Furthermore, the differential scattering cross section of x rays focused onto a charged particle system (liquid metal, plasma, or WDM) is determined by the DSF of the electrons [5]. This part is accessible via laboratory experiments using brilliant x-ray sources, generated by powerful optical lasers [6] or free electron lasers (FELs) [7]. The electron scattering spectrum has pronounced features in a wide range of energies. For instance, from the plasmon modes (having energies of several eV) one can derive the plasma parameters electron density n_e and electron temperature T_e using the detailed balance and the plasmon dispersion relation [5,8,9].

The correlations in the ion system are usually described via the static structure factor $S_{\mathrm{ii}}(k)$ applying classical integral equation techniques [10] or molecular dynamics (MD) simulations [11]. The ion acoustic modes (having energies of few 10 meV) can be resolved only using very intensive and narrow bandwidth radiation as provided by FELs [12]. The ion dynamics in WDM has been treated so far using MD simulations with respect to classical pair potentials [13] or applying orbital-free density functional theory [14] to calculate the forces in each time step. However, whether or not the ion dynamics in warm dense matter is described adequately by these approximate techniques remains an open question. In order to settle this point, we present here *ab initio* results for the DSF of the ions in liquid and, for the first time, also for warm dense Al using finite-temperature density functional theory molecular dynamics (DFT-MD) simulations.

The dynamic ion-ion structure factor $S_{\mathrm{ii}}(\vec{k},\omega)$ is defined as the Fourier transform of the intermediate scattering function $F_{\mathrm{ii}}(\vec{k},t)$,

$$F_{\mathrm{ii}}(\vec{k},t) := \frac{1}{N}\lim_{T\to\infty}\frac{1}{T}\int_0^T n_{\vec{k}}(\tau)n_{-\vec{k}}(\tau+t)d\tau, \qquad (1)$$

$$S_{\mathrm{ii}}(\vec{k},\omega) := \frac{1}{2\pi}\int_{-\infty}^{\infty} F_{\mathrm{ii}}(\vec{k},t)e^{i\omega t}dt, \qquad (2)$$

with $n_{\vec{k}}(t)=\sum_{i=1}^{N} e^{-i\vec{k}\vec{r}_i(t)}$ being the Fourier transformed ion number density and N the number of ions. For the calculation of $S_{\mathrm{ii}}(\vec{k},\omega)$ the ion movement is extracted from DFT-MD simulations using the Vienna Ab-Initio Simulation Package (VASP) [15–17]. For the inclusion of exchange interactions and correlations we use the generalized gradient approximation of Perdew, Burke and Ernzerhof [18]. The electron wave functions are expanded into plane waves up to a cutoff energy of 500 eV. For the interaction between ions and electrons a projector augmented-wave potential [19] is used, in which the ten inner electrons of Al atoms are frozen, while the three valence electrons are described in the DFT framework. All MD simulations except one were carried out using 256 ions and

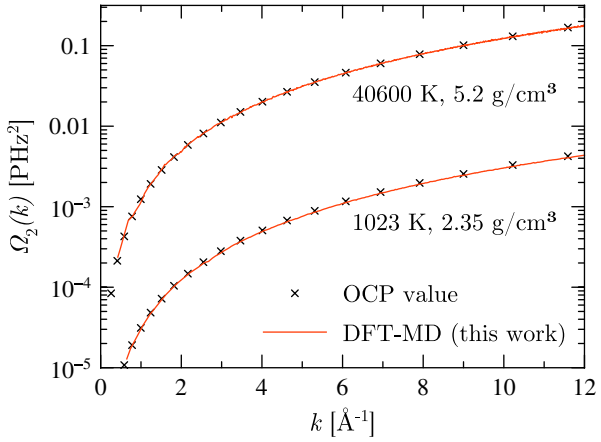

FIG. 1 (color online). Second frequency moments for aluminum from DFT-MD simulations (lines) compared with the OCP values (crosses). Lower curve: 1023 K and 2.35 g/cm^3, upper curve: 40 600 K and 5.2 g/cm^3.

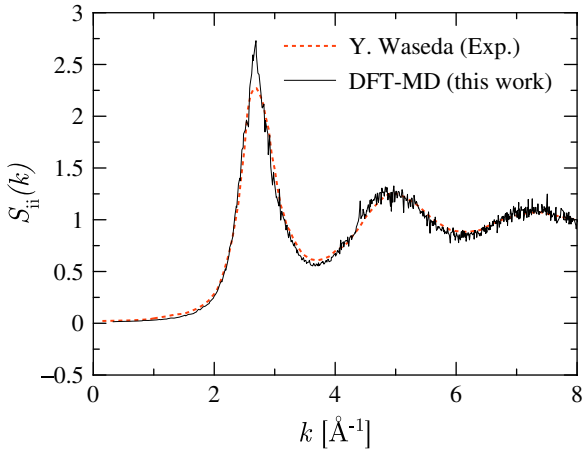

FIG. 2 (color online). Static structure factor $S_{ii}(k)$ at 1023 K and 2.35 g/cm^3 from x-ray diffraction experiments [22] (red dashed line) and DFT-MD simulation (black solid line).

ran for a minimum of 4400 time steps after equilibration. The time steps used in the ion dynamics part of VASP are 3 fs for Al near the melting point and 0.7 fs in the warm dense region. To control the temperature the algorithm of Nosé [20] is used with a Nosé mass corresponding to a temperature oscillation period of about 40 time steps. In all simulations the standard deviation of the temperature is between 5 and 10% of the mean value.

In general the form of the simulation box should correspond to the solid lattice structure of the material in question, allowing for possible solid-liquid transitions. The lattice structure of aluminum is fcc; therefore, we spanned the simulation box by using one short fcc vector $a(1,0,1)$ and two long fcc vectors $a(2,2,0)$ and $a(0,2,2)$. The constant a is then chosen according to the desired density. The sampling of the Brillouin zone was carried out at the Baldereschi mean value point [21] corresponding to the fcc simulation box. In the following only isotropic systems are considered; we therefore report only quantities averaged over the possible wave vectors with the same magnitude. The convergence of the results has been checked with regard to the number of particles, energy cutoff, Brillouin zone sampling, and the number of time steps. In order to check the accuracy of the method we determine the second frequency moment Ω_2 and compare with the theoretical value of the one component plasma (OCP) model $\Omega_2^{\mathrm{OCP}}(\vec{k}) = k_B T k^2/m$ in Fig. 1. The frequency moments are calculated from the intermediate scattering function (1) via

$$\Omega_n(\vec{k}) := \int_{-\infty}^{\infty} S_{ii}(\vec{k},\omega)\omega^n d\omega = (-i)^n \frac{\partial^n F_{ii}(\vec{k},t)}{\partial t^n}\bigg|_{t=0}. \quad (3)$$

The results of the DFT-MD simulations are in very good agreement with the OCP model (deviations less than 2 % for $k > 2$ Å^{-1}), thus validating the numerical treatment for this challenging problem.

The static structure factor $S_{ii}(k)$ is given by the intermediate scattering function (1) at time origin $F_{ii}(\vec{k},0)$. In Fig. 2 we compare our simulation results with available data from x-ray diffraction experiments [22] at 1023 K. Both are in very good agreement except for values at the first peak—a behavior that has already been observed in earlier MD simulations [23] for liquid metals near the melting point; it is caused by the periodic boundary conditions inducing additional order.

Ma *et al.* [24] recently measured the ion feature of shock-compressed aluminum with an estimated ion density of 0.181 Å^{-3} (mass density of 8.1 g/cm^3) and a temperature of 10 eV (116 000 K) via x-ray Thomson scattering. This allows us to compare experimental and *ab initio* structure data in the WDM region as well. Due to the high computational efforts necessary at these conditions this particular simulation was carried out with 64 ions in a box spanned by three fcc vectors of equal length. According to Chihara [25] the ion feature is given by

$$|f_i(k) + \rho(k)|^2 S_{ii}(k,\omega), \quad (4)$$

where $f_i(k)$ is the ion form factor and $\rho(k)$ the Fourier transform of the electron screening cloud. Both quantities are not accessible in our calculations; instead we approximate them by the atomic form factor [26]

$$f_i(k) + \rho(k) \approx f_a(k). \quad (5)$$

The resulting ion feature is in very good accordance with experimental data for large k; see Fig. 3. Ma *et al.* argue that only calculations taking into account the linear screening caused by free electrons as well as the short range repulsion which is due to bound electrons are able to reproduce their experimental data. This was shown by solving the

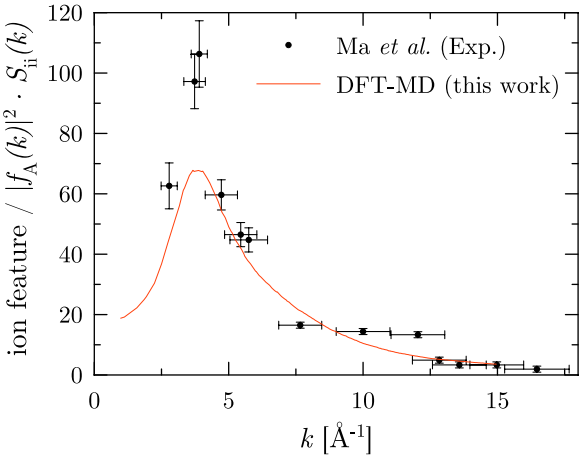

FIG. 3 (color online). Ion feature at 10 eV and 8.1 g/cm^3 from DFT-MD simulations (solid line) compared with the x-ray Thomson scattering data of Ma *et al.* [24] (dots).

Ornstein-Zernike equation within the hypernetted chain closure with respect to a potential that includes screening (Yukawa potential) and an appropriate but arbitrary short-range repulsion term (HNC − Y + SRR) [27]. This corresponds to the results of our calculations, where the height of the peak is underestimated due to the lack of a full quantum mechanical description of the ten inner shell electrons. Nevertheless, for the DSF of warm dense Al we investigate a system of lower density and temperature where the influence of Pauli blocking is expected to be smaller.

For the determination of $S_{ii}(\vec{k},\omega)$ we first calculate the intermediate scattering function $F_{ii}(\vec{k},t)$. This function still exhibits some statistical fluctuations after decaying; therefore we first multiply it with a Gaussian window function $e^{-t^2/(8t_{max}^2)}$ and then carry out the integration in Eq. (2) on the interval $[-t_{max},t_{max}]$. By this procedure we suppress the unphysical statistical fluctuations and reduce truncation effects. The value of t_{max} has to be chosen according to the decay time of $F_{ii}(\vec{k},t)$ and thus varies with the wave number k.

To test this method first calculations were performed for conditions matching those in the experiment of Scopigno *et al.* [28]. They investigated liquid aluminum at a temperature of 1000 K under ambient pressure. They did not report on the probe density; we therefore use the linear regression result from Ref. [29] leading to an average ion number density $n = 0.0526$ Å^{-3} (mass density of 2.3565 g/cm^3). In the experiment the static structure factor was not directly accessible and hence the normalization of the data has been determined by fitting procedures. The static structure factor in our calculations is by a factor of 1.65 greater than the values determined in Ref. [28]. In Fig. 4 we have used this factor to rescale the experimental data and compare with our simulation results. Since only wave vectors on the reciprocal lattice corresponding to the periodic boundary conditions are allowed

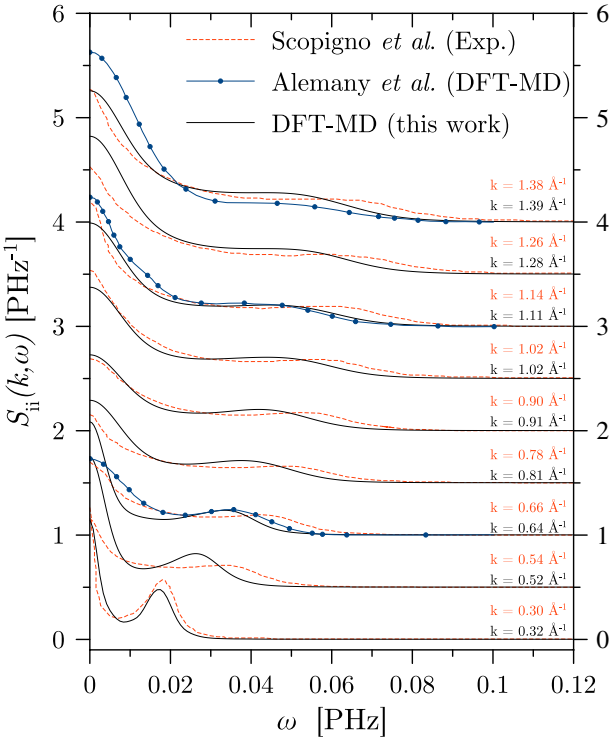

FIG. 4 (color online). DSF $S_{ii}(\vec{k},\omega)$ at 1000 K and 2.3565 g/cm^3. Dashed lines: experimental data from x-ray scattering [28]. Solid lines with dots: DFT-MD of Alemany *et al.* [30]. Solid lines: present DFT-MD. The lower wave numbers always correspond to the present DFT-MD, while the upper ones correspond to Ref. [28] and [30]. Each set of curves is shifted by a constant offset of 0.5 PHz^{-1} with respect to the lower one.

we compare at those wave numbers that are closest to the experimental ones.

An *ab initio* simulation for these conditions has already been carried out by Alemany *et al.* [30]. Our simulation

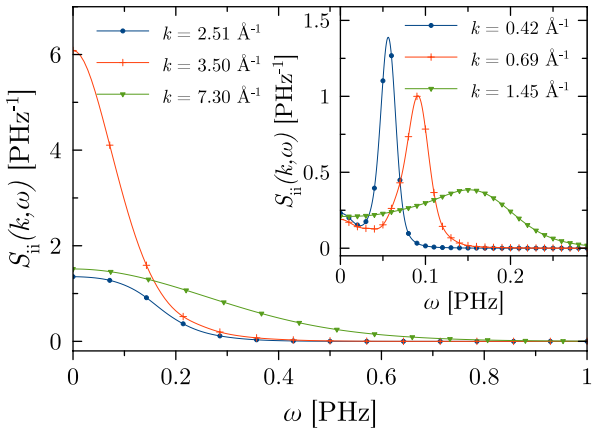

FIG. 5 (color online). DSF $S_{ii}(\vec{k},\omega)$ at 3.5 eV and 5.2 g/cm^3 from DFT-MD simulation. The wave vectors at 3.5 and 7.3 Å^{-1} correspond to the positions of the peaks in the static structure factor.

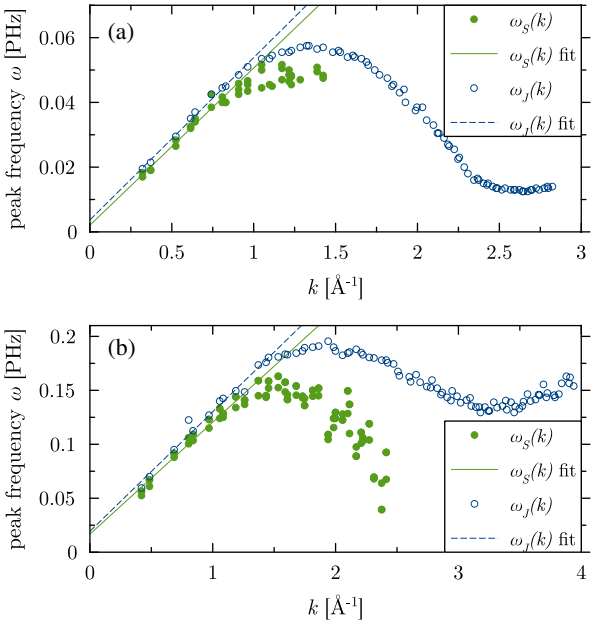

FIG. 6 (color online). Dispersion relation for ion acoustic modes. (a) Liquid aluminum at 1000 K and 2.3565 g/cm^3. (b) Warm dense aluminum at 40 600 K and 5.2 g/cm^3. Circles: dispersion relation from the positions of the side peaks of the DSF $S_{ii}(\vec{k},\omega)$. Dots: dispersion relation of the peaks of the longitudinal current correlation function $J_l(\vec{k},\omega)$.

uses a larger energy cutoff, a larger number of ions, a smaller time step and a larger number of time steps—which likely leads to more precise results. Alemany *et al.* report on the fraction $S_{ii}(\vec{k},\omega)/S_{ii}(\vec{k})$; therefore, in Fig. 4 we scaled their data according to our $S_{ii}(\vec{k})$ values. At all points our simulation and the experiment show very good agreement. However, the position of the side peaks is slightly lower in the simulation, a circumstance also present in the calculations of Alemany *et al.*

For the investigation of the DSF of warm dense aluminum we chose a temperature of 3.5 eV (40 600 K) and an ion number density of $n = 0.116$ Å^{-3} (mass density of 5.2 g/cm^3). In Fig. 5 we show results for the DSF at the peaks of the static structure factor and in the collective region. Compared to the case near the melting point the collective modes are much more pronounced. This is a consequence of the strong correlations inherent in WDM states.

For the two cases studied in this work the dispersion relation of the collective excitations has been determined analyzing the position of the side peaks; see Fig. 6. The peak positions depends on the choice of t_{max} in the window function. Since there is no strict rule for the choice of t_{max}, we include results from different choices of t_{max} in our calculations.

The slope of the dispersion relation for small wave vectors is the adiabatic sound velocity c_s. We report also on the dispersion relation of the longitudinal current correlation spectra $J_l(\vec{k},\omega) = \omega^2/|\vec{k}|^2 S(\vec{k},\omega)$, where the slope at small wave vectors gives the apparent sound velocity c_l. For all dispersion relations the corresponding sound velocities have been determined via linear fits to the dispersion relation at small wave vectors, see Table I.

TABLE I. Adiabatic and apparent sound velocity for liquid (1000 K, 2.3565 g/cm^3) and warm dense aluminum (40 600 K, 5.2 g/cm^3).

T (K)	ϱ (g/cm^3)	c_s (m/s)	c_l (m/s)
1000	2.3565	4860	5010
40 600	5.2	10 380	11 070

For liquid aluminum at 1000 K an adiabatic sound velocity of 4722 m/s can be estimated from experimental data [31]. Our DFT-MD results for the sound velocities agree within 6 %. Furthermore, we give first predictions for the sound velocities in warm dense aluminum which are about a factor two greater than those in the liquid metal regime. Such a noticeable increase of c_s has already been found in orbital-free DFT-MD [14] at slightly different conditions, and in DFT-MD results for warm dense hydrogen along the Jupiter isentrope as well [3].

In summary, *ab initio* simulations were shown to be a reliable tool to describe the dynamics of liquid metals near melting. We applied this method for the first time to compute the ion dynamics in the WDM region with its strong correlations and quantum effects. We have shown that collective excitations play a dominant role there. From the dispersion relations of these ion acoustic modes, the sound velocities have been derived, being in good accordance with experimental data. Results on the ion feature of warm dense aluminum [24] show good agreement for the large-k region and support the assumption that short range repulsions between the ions have a strong influence on the measured peak height. Our results are very encouraging for a full *ab initio* description of the structural properties of WDM, that should be based on an all-electron DFT calculation.

We thank Th. Bornath, S. H. Glenzer, G. Gregori, W. Lorenzen, P. Neumayer, K.-U. Plagemann, and T. G. White for helpful discussions. We thank the DFG for support within the SFB 652.

[1] W. Kraeft, D. Kremp, W. Ebeling, and G. Röpke, *Quantum Statistics of Charged Particle Systems* (Akademie-Verlag, Berlin, 1986).
[2] N. Nettelmann, A. Becker, B. Holst, and R. Redmer, Astrophys. J. **750**, 52 (2012).
[3] M. French, A. Becker, W. Lorenzen, N. Nettelmann, M. Bethkenhagen, J. Wicht, and R. Redmer, Astrophys. J. Suppl. Ser. **202**, 5 (2012).
[4] J. Lindl, Phys. Plasmas **2**, 3933 (1995).

[5] S. H. Glenzer and R. Redmer, Rev. Mod. Phys. **81**, 1625 (2009).
[6] A. L. Kritcher, P. Neumayer, J. Castor, T. Döppner, R. W. Falcone, O. L. Landen, H. J. Lee, R. W. Lee, E. C. Morse, A. Ng, S. Pollaine, D. Price, and S. H. Glenzer, Science **322**, 69 (2008).
[7] U. Zastrau *et al.*, Laser Part. Beams **30**, 45 (2012).
[8] S. H. Glenzer, O. L. Landen, P. Neumayer, R. W. Lee, K. Widmann, S. W. Pollaine, R. J. Wallace, G. Gregori, A. Höll, T. Bornath, R. Thiele, V. Schwarz, W.-D. Kraeft, and R. Redmer, Phys. Rev. Lett. **98**, 065002 (2007).
[9] R. Thiele, T. Bornath, C. Fortmann, A. Höll, R. Redmer, H. Reinholz, G. Röpke, A. Wierling, S. H. Glenzer, and G. Gregori, Phys. Rev. E **78**, 026411 (2008).
[10] K. Wünsch, J. Vorberger, G. Gregori, and D. O. Gericke, Europhys. Lett. **94**, 25001 (2011).
[11] D. Schiff, Phys. Rev. **186**, 151 (1969).
[12] G. Gregori and D. O. Gericke, Phys. Plasmas **16**, 056306 (2009).
[13] J. P. Hansen, I. R. McDonald, and E. L. Pollock, Phys. Rev. A **11**, 1025 (1975).
[14] T. G. White, S. Richardson, B. J. B. Crowley, L. K. Pattison, J. W. O. Harris, and G. Gregori, Phys. Rev. Lett. **111**, 175002 (2013).
[15] G. Kresse and J. Hafner, Phys. Rev. B **47**, 558 (1993).
[16] G. Kresse and J. Hafner, Phys. Rev. B **49**, 14251 (1994).
[17] G. Kresse and J. Furthmüller, Phys. Rev. B **54**, 11169 (1996).
[18] J. P. Perdew, K. Burke, and M. Ernzerhof, Phys. Rev. Lett. **77**, 3865 (1996).
[19] P. E. Blöchl, Phys. Rev. B **50**, 17953 (1994).
[20] S. Nosé, J. Chem. Phys. **81**, 511 (1984).
[21] A. Baldereschi, Phys. Rev. B **7**, 5212 (1973).
[22] IAMP database of [SCM-LIQ], originally published in Y. Waseda, *The Structure of Non-Crystalline Materials* (McGraw-Hill, New York, 1980), http://res.tagen.tohoku.ac.jp/~waseda/scm.
[23] J. A. Anta, B. J. Jesson, and P. A. Madden, Phys. Rev. B **58**, 6124 (1998).
[24] T. Ma, T. Döppner, R. W. Falcone, L. Fletcher, C. Fortmann, D. O. Gericke, O. L. Landen, H. J. Lee, A. Pak, J. Vorberger, K. Wünsch, and S. H. Glenzer, Phys. Rev. Lett. **110**, 065001 (2013).
[25] J. Chihara, J. Phys. Condens. Matter **12**, 231 (2000).
[26] J. H. Hubbell, W. J. Veigele, E. A. Briggs, R. T. Brown, D. T. Cromer, and R. J. Howerton, J. Phys. Chem. Ref. Data **4**, 471 (1975).
[27] K. Wünsch, J. Vorberger, and D. O. Gericke, Phys. Rev. E **79**, 010201 (2009).
[28] T. Scopigno, U. Balucani, G. Ruocco, and F. Sette, Phys. Rev. E **63**, 011210 (2000).
[29] M. J. Assael, K. Kakosimos, R. M. Banish, J. Brillo, I. Egry, R. Brooks, P. N. Quested, K. C. Mills, A. Nagashima, Y. Sato, and W. A. Wakeham, J. Phys. Chem. Ref. Data **35**, 285 (2006).
[30] M. M. G. Alemany, L. J. Gallego, and D. J. González, Phys. Rev. B **70**, 134206 (2004).
[31] S. Blairs, Int. Mater. Rev. **52**, 321 (2007).